Bioconjugate Chemistry

Subscriber access provided by University of Leicester

Communication

Complete Generation of a Xe Biosensor on the Solid Support by Systematic Backbone Assembly

Jabadurai Jayapaul, and Leif Schröder

Bioconjugate Chem., **Just Accepted Manuscript** • DOI: 10.1021/acs.bioconjchem.8b00814 • Publication Date (Web): 14 Nov 2018

ACS Publications

is published by the American Chemical Society. 1155 Sixteenth Street N.W., Washington, DC 20036

Complete Generation of a ^{129}Xe Biosensor on the Solid Support by Systematic Backbone Assembly

Jabadurai Jayapaul* and Leif Schröder*

Molecular Imaging, Department of Structural Biology, Leibniz-Forschungsinstitut für Molekulare Pharmakologie, Robert-Rössle-Str.10, 13125 Berlin, Germany

E-mail: jayapaul@fmp-berlin.de; lschroeder@fmp-berlin.de

Phone: +49 (0)3094793 121. Fax: +49 (0)3094793 189

Abstract

Xenon biosensors are an emerging tool for different molecular imaging applications. For many applications, their development requires peptide synthesis steps, followed by the selective installation of a xenon host onto the peptide backbone in solution. In this study, three different strategies were attempted for generating the entire Xe biosensors on the solid support. Notably, one strategy involving CryA-da was beneficial by directly integrating this host into the growing construct on a low loaded resin via modification of the administered sub-component equivalents and by prolonging the coupling procedure. Subsequently, installation of additional amino acids or of additional labels onto the growing construct was achieved by a procedure in which an excess amine was administered to the activated CryA-da (acid) anchored onto the resin. Further, the as-generated Xe biosensor was tested for its NMR and MRI capabilities in H_2O and compared to the performance of CryA-ma. Xe NMR of the biosensor indicated a clear CEST response and the Xe MR images revealed similar contrast compared to the

reference host. These observations suggest that functionalizing CryA-da on both sides with multiple labels did not alter significantly its NMR capabilities. Hereby, we could show the successful and complete synthesis of a CryA-da-based xenon biosensor on the solid support without any notable side reactions and without the necessity of multiple purification steps.

Introduction

Solving the sensitivity issue of NMR and MRI through the design of reporters that make optimized use of the available magnetization is an active field of research. In this context, spin hyperpolarization is an emerging technique that requires strategies to incorporate certain nuclei such as ^{13}C and ^{15}N into biomolecules of diagnostic interest to detect enhanced magnetization after applying methods such as dynamic nuclear polarization (DNP) or para-hydrogen induced polarization (PHIP).[1–4] Another approach is based on hyperpolarized ^{129}Xe that can be functionalized for sensing purposes.[5,6] This requires incorporation of the NMR-active nuclei in a different way since the noble gas is not covalently bound to any molecules of biological relevance. Xe is rather transiently trapped in a host structure that confers a distinct chemical shift to the nuclei upon binding. This feature allows to combine two signal amplification schemes: spin hyperpolarization achieved through spin exchange optical pumping (SEOP) and indirect detection based on chemical exchange saturation transfer (CEST). Hyperpolarized ^{129}Xe that is associated with the host-bearing reporter molecule through reversible formation of host-guest complexes can be detected through the Hyper-CEST method.[6] Thus, the critical labelling step is the incorporation of an entire host structure rather than of an NMR-active isotope itself. Once achieved, this allows encoding of many transiently bound Xe atoms while they exchange in and out of the pool of free Xe.

A robust macrocycle as host is necessary such that it can trap Xe momentarily and can provide a handle for further chemical modification (typical hosts are, e.g., crytophanes, cucurbit[n]urils, or pillar[n]arenes etc.).[7–10] Among the macrocycles, crytophanes display a good

binding affinity for Xe in addition to exhibiting moderate Xe exchange rates. Cryptophane-A (CryA) with one or two carboxylic acid groups (CryA-ma and CryA-da, see Fig. 1A) has been used in various studies to design Xe biosensors. Like for other imaging modalities, e.g., fluorescence imaging, it is a common strategy to couple the host as a functional unit to peptidic backbones or to shorter units that are grafted onto larger scaffolds (e.g., viral capsids, phages[11–13]). An important aspect is to minimize side products that could arise during or after incorporation of the CryA unit. Previous approaches have been performed in solution with final attachment of the host that itself requires an elaborate synthesis. Here, we investigate three different approaches to couple a CryA unit to a backbone on the solid support in combination with a fluorescent reporter unit (5(6)-Carboxyfluorescein) and an exemplary binding moiety (biotin).[11,14,15] We particularly discuss the challenges that come with crowding effects, either arising at neighboring side chains when introducing bulky units with short handles (a common aspect of CryA building blocks), or occurring with highly loaded resins (see Fig. 1B). While extended peptides might help to avoid steric hindrance, our strategy aims to avoid unnecessary long peptides because this increases the risk for interactions of the peptide tail with the attached cage. Such interactions may block Xe access to the cavity—an effect observed by us and others[16,17] for which the exact mechanism has not yet been fully understood.

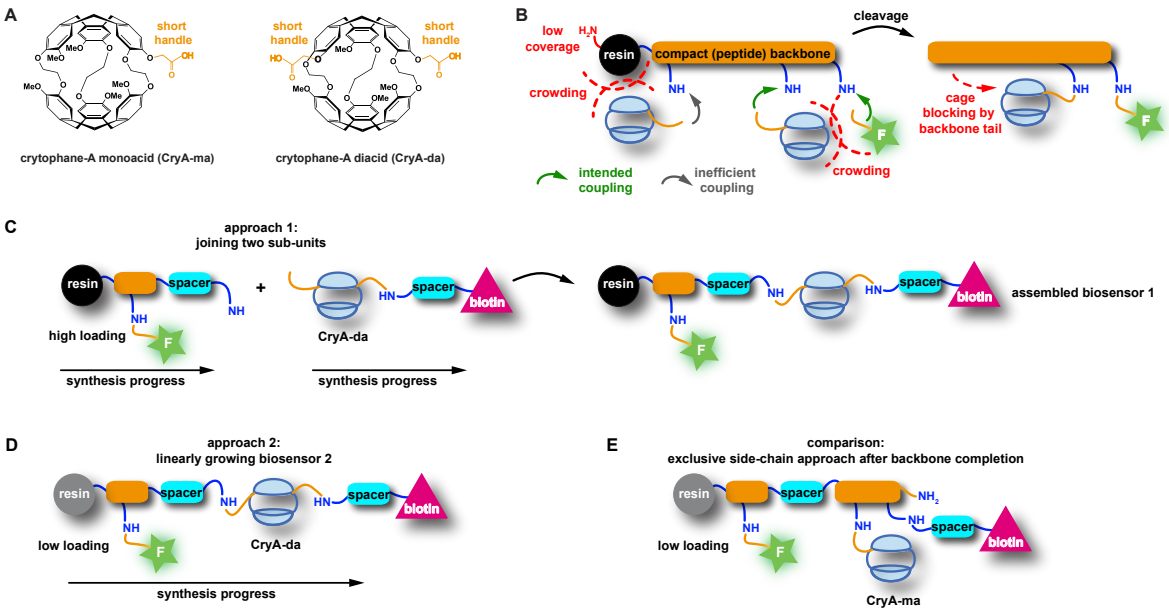

Figure 1. Scheme illustrating challenges and different synthetic routes for ^{129}Xe biosensors. (A) Chemical structures of Xe hosts used in this study with their short coupling handles. (B) Possible challenges (highlighted in red) include limited reactivity at intended coupling sites due to crowding at side chains when attaching bulky functional units; low coverage of the resin might be inevitable if coupling of such bulky units is attempted too close to the resin; blocking of the cage through the peptide tail might occur after cleavage. (C) A fluorophore-tagged peptide backbone sub-component generated on a high loaded resin was subsequently combined on the resin with CryA-ma-biotin sub-component synthesized in solution. (D) Joining different labels along a linearly growing backbone on a low loaded resin support. (E) Peptide backbone built on a low loaded resin and finally loaded with different labels (e.g., fluorophore, CryA-ma and biotin) via the side chain.

CryA possesses three ethylenic ether linkages for connecting two cyclotriveratrylene (CTV) hemispheres which both consist of three methoxy-substituted, methylene-bridged phenyls that are responsible for entrapping Xe (Fig. 1A).[18] Replacing one or multiple methoxy groups of CryA with a short carboxyl or propargyl handle for further substitution or coupling is a common strategy. Preferably, all coupling steps are performed on a resin to allow excess reagents and side products being removed by washing and filtration. However, accessibility of reactive groups might be problematic in this case. Some approaches achieved coupling of monopropargyl-CryA to an azidopeptide on a solid support via Cu(I)-catalyzed [3 + 2] azide-alkyne cycloaddition.[19,20] Noteworthy, that approach cleaved the peptide from the resin before the last functional unit (the Cy3) was attached in order to avoid steric hinderance among the different labels (e.g., bulky CryA, targeting unit, and fluorophore;

see Fig. 1B). The steric issue persisted nonetheless in that approach and led to reduced coupling efficiency of the fluorophore onto the peptide. Introduction of multiple units could be facilitated by providing longer handles on, e.g., the cage. However, this could lead to aggregation of the cage units[21] prior to coupling and the cage as a sensing unit would also get to far away from the targeting unit that interacts with the analyte.

Circumventing such issues would make a growing (peptidic) backbone the preferred way to incorporate all desired units. CryA-ma could be part of such a synthesis by attaching it to a Lys side chain or at the *N*-terminus but the challenge is to enable a protocol on a solid support where the introduction of each unit does not impede one of the later coupling steps. Alternative approaches have been introduced where the Xe host itself serves as a scaffold for attaching multiple units: trifunctionalization[22] or hexafunctionalization[23] of CryA have been proposed for improving the targeting efficiency of Xe biosensors. However, such approaches are prone to yield a mixed functionalization of CryA upon coupling to different reporters. To avoid later functionalization hurdles, we pursued a strategy in which the host is incorporated into a growing backbone such that crowding between neighboring side chain units is avoided. This is achievable using CryA-da with minimal functionalization complexity. Our example serves as a model system for obtaining Xe biosensors with defined distribution of functional moieties on the solid support.

Results and discussion

Choice of the model sensor for this study was motivated by a previously introduced concept in which biotin is used as a unit to enable binding to avidin-tagged antibodies.[24] Such an approach allows for "modular" biosensors that can easily be adapted to different biological targets. Hence, the synthesis has to join biotin, the Xe host, and a fluorescence reporter as essential units. Originally, the construct was synthesized by irradiating CryA-da with microwave after providing equimolar subcomponents with biotin and fluorophore units, re-

spectively. This approach led to very low yields (ca. 10 %) owing to formation of various side products. The aim of this study was thus to establish a protocol in which CryA-da is incorporated into the growing construct on the resin in order to have good control over the products and avoid "incomplete" constructs where, e.g., the Xe host is installed but the fluorophore is missing.[25]

To do so, primarily two different synthetic strategies for obtaining the desired construct from CryA-da were investigated as shown in Table 1 and Fig. 1C/D, respectively. In the first strategy, two building blocks of the model biosensor **(1)** were synthesized separately, followed by joining the as-generated sub-components efficiently on the solid support (see Fig. 1C). Such strategy was considered to be beneficial for obtaining higher yields and also for promoting the CryA-da functionalization with different labels at ease. To test our strategy, the synthesis of two sub-components (**(1a)** and **(1b)**, SI section 4.1) of the final construct was pursued as follows: sub-component **(1a)** was generated by activating CryA-da using DCC/NHS followed by coupling the crude CryA-da di-NHS ester to lower equivalents of $H_2N{-}CH_2CH_2(PEG)_3{-}$biotin in solution (Fig. 2). The desired sub-component **(1a)** was isolated with 10% yield after HPLC purification (Fig. S6) and subsequent MALDI-MS analyses (Fig. S1).

Table 1. List of model Xe biosensors. The introduced Xe host units are highlighted in bold. While **1** and **2** aim to avoid crowding at neighboring side chains, **3** was attempted for comparison.

Entry	model Xe biosensors
1	Biotin-$(PEG)_3CH_2CH_2$-**(CryA-da)**-$(PEG)_3CH_2CH_2$-Lys(5/6-FAM)-Gly
2	Biotin-$(PEG)_3CH_2CH_2$-**(CryA-da)**-$(PEG)_3CH_2CH_2$-Lys(5-FAM)
3	Acetyl-Glu((PEG)$_3$biotin)-Lys**(CryA-ma)**-$(PEG)_3CH_2CH_2$-Lys(5/6-FAM)-Gly

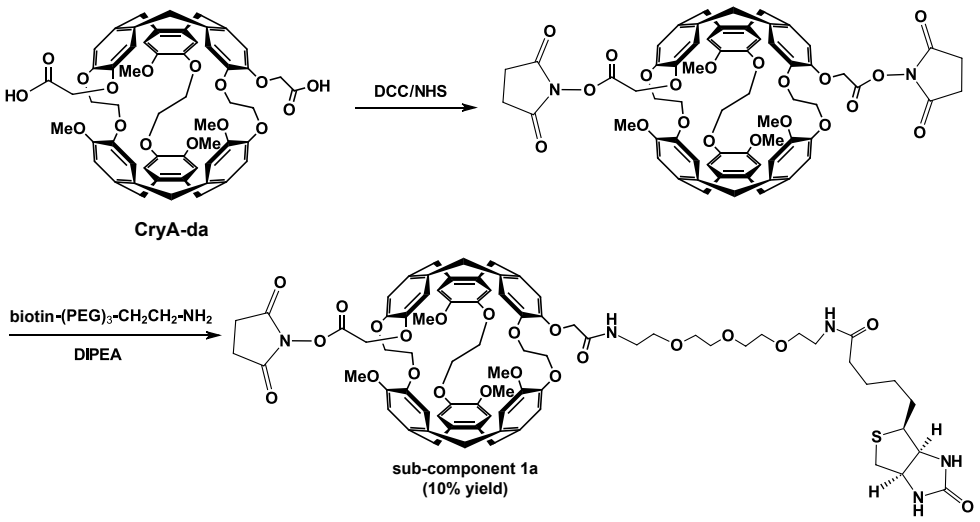

Figure 2. CryA-da was derivatized using DCC/NHS to yield di-*N*-succinimidyl ester of CryA-da prior to its coupling to biotin$-(PEG)_3CH_2CH_2-NH_2$ to generate the biosensor sub-component **(1a)**.

The other sub-component **(1b)** was synthesized using a glycine-preloaded Wang® resin (SI section 4.1). A fluorophore-tagged lysine building block and a PEG spacer were conjugated to the glycine anchored on the resin. Fmoc deprotection was monitored by UV absorption and by Kaiser's test for free amines prior to each coupling step performed for this and the other sensors on the resin. The generation of **(1b)** was confirmed by MALDI-MS analysis (Fig. S2) after cleavage and HPLC purification. However, the HPLC analysis of crude **(1b)** indicated less efficient coupling and low yields (Fig. S7). This observation could be attributed to lower surface coverage of the highly (pre-)loaded Wang® resin, a consequence emerging from inevitable administration of lower equivalents of the bulky Lys(5/6-FAM) building block. Extending the peptide on the resin before attaching the dye unit with higher coverage was not pursued here because of the above mentioned reasons.

Eventually, such inefficient coverage of the preloaded resin in the initial coupling step might influence the overall coupling of **(1a)** with **(1b)** (depicted in Fig. 3) if a rather unwanted high reactivity of **(1a)** with activated Gly occurs. Combining the two sub-components on the resin resulted indeed only in partial conjugation (Fig. S3). Even after prolonging the reaction time, the final conjugation did not proceed to completion. A

possible alternative would be to employ a resin with low loading and to perform the final conjugation of both sub-components in solution such that the issue of reduced resin surface coverage could be avoided. Additionally, monoprotected CryA-da would be highly beneficial to specifically tether the labels in higher yields and for promoting its easy conjugation to the growing construct on the resin.

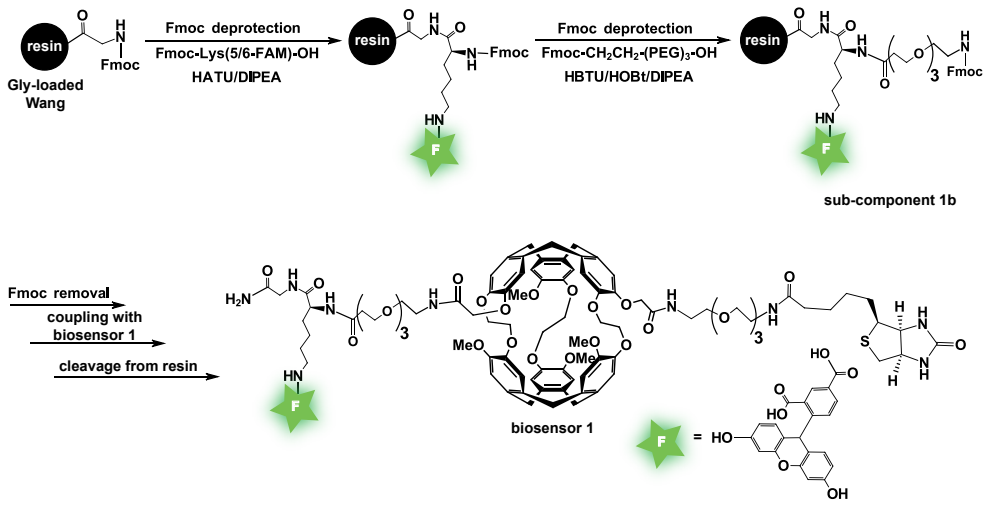

Figure 3. A high Gly-loaded Wang® resin was grafted with the Fmoc-Lys(5/6-FAM)-OH and Fmoc$-CH_2CH_2(PEG)_3-$OH using appropriate coupling reagents under basic conditions to form the biosensor sub-component **(1b)**. Then, both biosensor sub-components **(1a & 1b)** were joined together on the solid support to generate the final biosensor **(1)**.

Instead of implementing such modifications in the synthesis, we decided to pursue an alternative strategy. Nonetheless, the insights gained from this initial approach were favorable for generating the model biosensor **(2)** entirely on the solid support. In this second strategy, the synthesis was attempted by using lower equivalents of unprotected CryA-da such that it can be linearly inserted into the growing construct on the resin and also for enabling further functionalization with different labels (Fig. 1D). Tentagel R RAM® resin with low loading was utilized for generating the biosensor **(2)** such that issues related to lower surface coverage were averted (SI section 4.2). After Fmoc-deprotection of the resin, Fmoc-Lys(Dde)-OH was anchored onto the resin by HATU-mediated prolonged coupling, followed by the installation of a PEG spacer. Subsequently, a sub-equivalent of unprotected CryA-da was provided to

the growing construct on the resin in order to lessen the cross reactivity of CryA-da with the preceding amino acid residue. This critical coupling was facilitated by double and HATU-mediated extended coupling. It is anticipated that the interference of backbone fraction without CryA-da label on subsequent coupling steps with additional labels is minimal since the administered equivalents of new labels are based on submillimolar ratios of the coupled CryA-da. To our knowledge, this is the first demonstration of a selective coupling of one of the two equally reactive acid groups of a macrocyclic Xe host to the *N*-terminus of a peptide on the solid support.

Next, the activation of the uncoupled acid group of CryA-da was achieved using DCC/NHS under dry solvent conditions. Contrary to conventional peptide synthesis, a 2-fold excess of PEG-biotin (amine) was utilized for coupling it to NHS-activated CryA-da (acid) of the anchored peptide. HPLC analysis at this stage revealed the successful synthesis of the peptide backbone (Fig. S8). Consecutively, the Dde protection group was removed from the lysine side chain and the fluorophore (5-carboxyfluorescein) was selectively installed using HATU-mediated prolonged coupling. MALDI-MS analysis proved the successful synthesis of biosensor **(2)** (Fig. S4) according to Fig. 4. Since submillimolar equivalents of CryA-da and low loaded resin were utilized for synthesizing **(2)**, an overall yield of about 20% was achieved for the final construct. This is practically twice the yield of the original synthesis in solution. In this way, we could demonstrate that a synthetically challenging compact sequence for Xe biosensors comprising multiple labels can be successfully and completely synthesized on the solid support. Comparison of the results from synthesis pathways of **(1)** and **(2)** illustrates that the step-wise addition of individual units starting from a low loaded resin allows efficient incorporation of all functional groups even if the bulky host, the fluorophore, and the targeting unit are in relative close proximity.

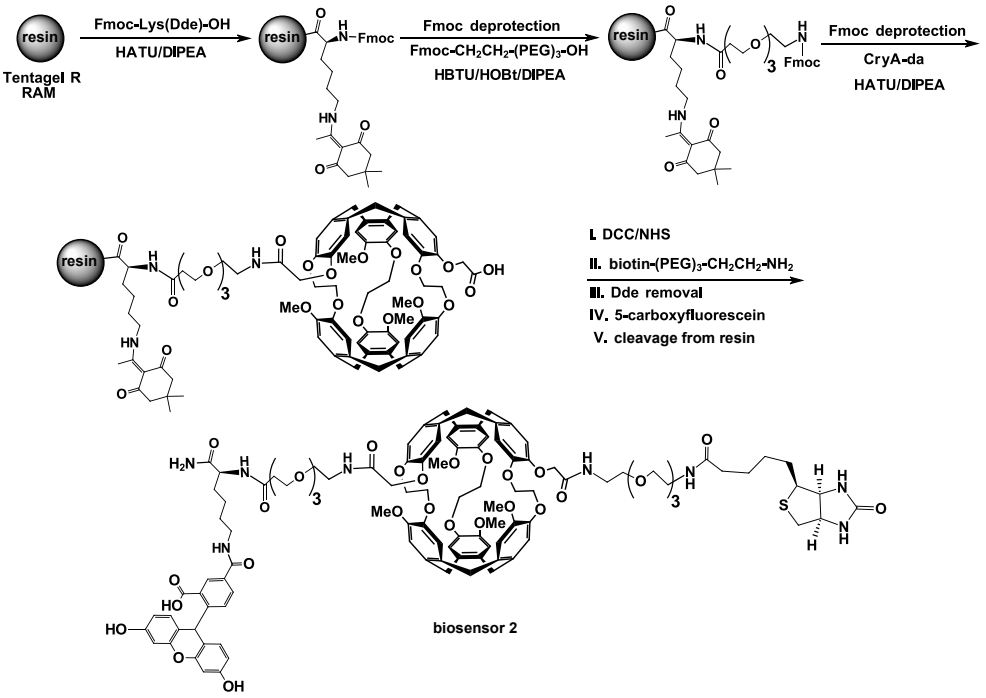

Figure 4. Synthesis steps involved in the generation of biosensor **(2)** on the solid support. Fmoc-Lys(Dde)-OH was anchored to low loaded Tentagel® resin and then the former was conjugated to Fmoc$-CH_2CH_2(PEG)_3$OH. CryA-da was linearly inserted into the peptide by administering sub-millimolar equivalents. Subsequently, mono-NHS derivatizated CryA-da was coupled to biotin$-(PEG)_3CH_2CH_2NH_2$, followed by the attachment of the fluorophore tag onto the lysine side chain while the peptide was still connected to the resin.

We further investigated if a similar sensor would be achievable based on CryA-ma. In analogy to other reporters, such strategy would have the potential advantage that the different functional units all come with only one reactive group and are introduced via the side chains of the completed (peptide) backbone (see Fig. 1E). However, to obtain desired final construct via this strategy, the interference emerging from administering lower amino acid or building block equivalents in a coupling step and undesired simultaneous deprotection of two protecting groups (e.g., Dde and Fmoc groups) should be avoided. Moreover, steric hinderance might become an issue once the different units shall all be installed on the complete compact backbone.

The model biosensor Acetyl-Glu((PEG)$_3$biotin)-Lys(CryA-ma)-(PEG)$_3$CH$_2$CH$_2$-Lys(5/6-FAM)-Gly **(3)** as shown in Table 1 was generated by HBTU- and HATU-mediated prolonged coupling under basic conditions. The reporter and targeting units were chosen to be system-

atically installed onto the side chains of the peptide backbone as shown in Fig. 1E. Tentagel R RAM® resin with low loading was utilized again for synthesis of the peptide backbone. The first amino acid (Fmoc-Gly(OtBu)-OH) was conjugated to the resin by subjecting it to HBTU/HOBt-mediated double coupling under basic conditions. Following the Gly-addition, the fluorophore was linked to the glycine by employing lower molar equivalents of fluorophore-containing amino acid building block, i.e., Fmoc-Lys(5/6-FAM)-OH, via prolonged HATU-mediated coupling. Consecutively, the PEG linker (Fmoc$-CH_2CH_2(PEG)_3-$OH), Fmoc-Lys(Dde)-OH and Fmoc-Glu(OtBu)-OH were coupled according to the synthetic protocols described under the supporting information (SI section 4.3).

Next, the free amine available at glutamic acid residue after Fmoc removal was acetylated to prevent undesired coupling of CryA-ma at this position. We then attempted to install CryA-ma after selective removal of Dde group from the lysine side chain at its ε-position (Fig. 5). However, repeated synthesis attempts led to unsuccessful coupling inferring unavailability of the free amine at the lysine residue as confirmed by HPLC and MALDI-MS analyses (Figure S9, S5). Such unsuccessful attempts might occur due to the acetylation procedure and the hopping nature of Dde protection group[26] among the free amine groups of different amino acids. A way around the acetylation and Dde protection issues is to install lysine with less interfering protecting group e.g., Fmoc-Lys(trt)-OH prior to Fmoc-Glu(OtBu)-OH. By doing so, CryA-ma can be tethered directly at the lysine after *trt* removal without the need for Fmoc deprotection followed by acetylation of glutamic acid. However, such approaches should be meted out in a way that it does not introduce any additional side reactions.

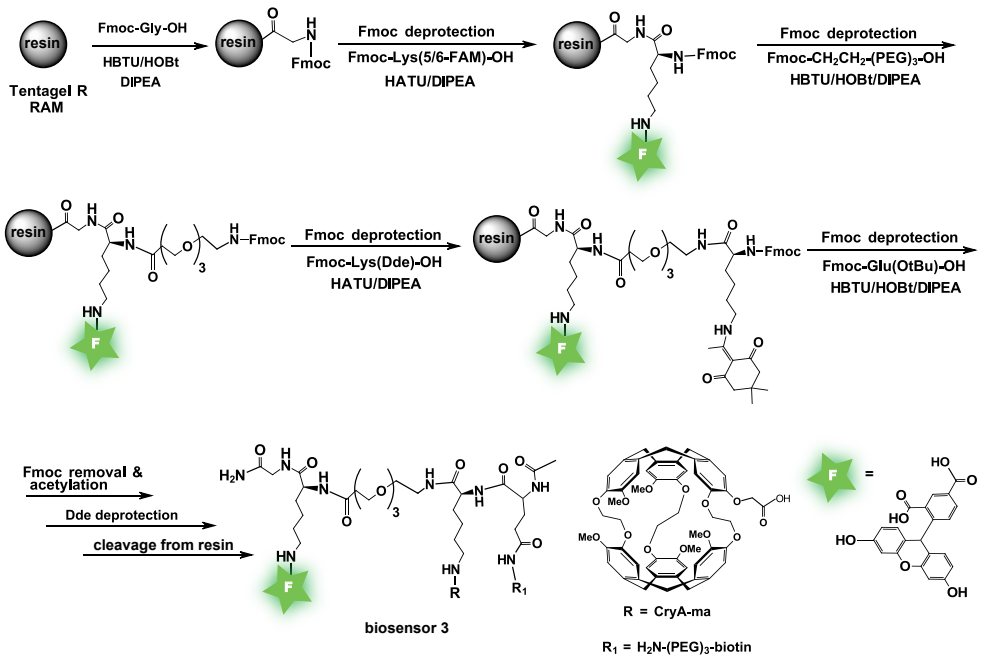

Figure 5. The synthetic scheme reveals different steps involved in the generation of biosensor **(3)**. The amino acids were anchored onto Tentagel R RAM® resin and coupled to other labels mainly using HBTU/HOBT reagents under basic conditions. Fmoc-Lys(5/6-FAM)-OH and Fmoc-Lys(Dde)-OH were installed on the growing peptide by HATU-mediated prolonged coupling. The free amine group in the glutamic acid after Fmoc removal was acetylated to prevent it from coupling to different labels (e.g., CryA-ma), respectively.

Altogether, the synthesis of a construct to be used for modular Xe biosensors was most successful for the strategy used for construct **(2)**, despite the challenges of joining multiple functional units in close proximity. This approach provided efficient control over the growing construct, straight forward handling of one protection unit at a time, and avoided mixed results as obtained in previous pathways performed in solution.

Finally, the ^{129}Xe-HyperCEST NMR capabilities of as-synthesized biosensor **(2)** were evaluated by utilizing 9.6 μM of **(2)** and CryA-ma as reference in H_2O containing 1 % DMSO and 0.1 % PL-81 (SI section 7). ^{129}Xe-HyperCEST (z-) spectra indicated CEST peaks at -131.2 ppm (biosensor **(2)**) and -132.4 ppm (CryA-ma) upfield from free Xe in solution (Fig. 6A). This supports the claim that the linear incorporation of CryA-da into the growing construct and subsequent functionalization with other units did not disable the Xe binding and the exchange in/out of CryA-da. However, the CEST response of **(2)**

was somewhat reduced and more narrow when compared to that of the uncoupled host (CryA-ma; illustrated by dashed lines at FWHM in Fig. 6A). This observation is in line with a potentially reduced exchange rate as a consequence of attaching other units in close proximity, which is supported by the reduced exchange rate observed for a similar biosensor system where CryA-da was tethered on both sides with second generation dendrimers (~ 23 s^{-1})) and compared to CryA-ma (~ 24 s^{-1}).[27] Another option to be considered is that **(2)** forms aggregates as recently reported for other CryA constructs.[21] Such aggregation could affect the exchange rate. We thus performed DLS measurements of **(2)** at 96 μM in 10% DMSO plus 1% PL-81 and observed a particle size of 227 ± 2 nm (Fig. S11). However, these particle sizes were also observed in the blank sample and are thus assigned to aggregates of the antifoam agent.

Subsequently, the imaging capabilities of both **(2)** and CryA-ma were tested in H_2O containing 1 % DMSO and antifoam A (0.05%) using ^{129}Xe-HyperCEST MRI (SI section 8). Here, a double phantom consisting of two NMR tubes placed one inside the other (thus forming two compartments) was utilized. Biosensor **(2)** was placed in the inner compartment while the CryA-ma was given into the outer one (Fig. 6B). To achieve ^{129}Xe-HyperCEST images, the samples were saturated "on-resonant" with the frequencies of two signals of bound Xe, *i.e.*, at -131.2 ppm and -132.4 ppm (Fig. 6D-E). This was complemented by a symmetric "off-resonant" saturation at -133.6 ppm (Fig. 6C; no signal averaging for any of the MRI scans). The obtained ^{129}Xe-HyperCEST images at $(32)^2$ pixels resolution for a $(10\ \text{mm})^2$ field of view visualize the signal intensities changes occurring among the images while applying different saturation frequencies (Fig. S12). Thus, we show that by choosing appropriate saturation conditions the full ^{129}Xe biosensor can be localized efficiently in par with Xe host while being separated by a small frequency difference (~ 1 ppm).

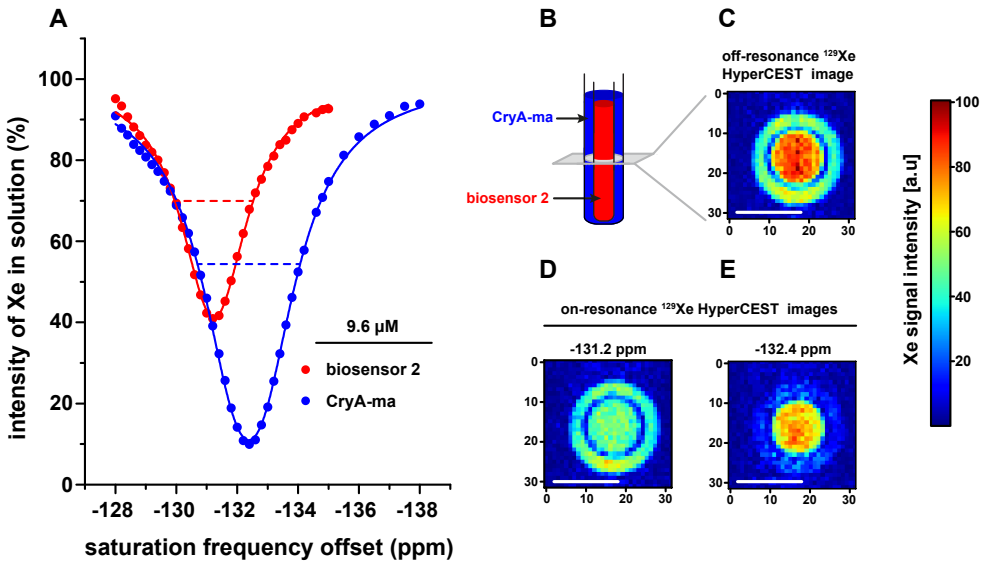

Figure 6. Evaluation of biosensor **(2)** in comparison to CryA-ma using ^{129}Xe HyperCEST NMR and MRI (A-E). A: ^{129}Xe HyperCEST (z-) spectra of biosensor **(2)** and CryA-ma at 9.6 μM in H_2O containing 1% DMSO indicated CEST peaks at -131.2 ppm (**(2)**) and -132.4 ppm, respectively. B: The schematic shows bubbling phantom used for ^{129}Xe HyperCEST MRI measurements in which **(2)** (9.6 μM in 1% DMSO) is placed in the inner compartment while the CryA-ma (9.6 μM in 1% DMSO) in the outer one. C: Representative slightly off-resonance ^{129}Xe HyperCEST image of both samples in the double phantom. D-E: On-resonance Xe HyperCEST images indicated that CryA-ma achieves more saturation transfer than **(2)** which is in strong agreement with the spectral observations. Scale bar used in the image is 5 mm.

Conclusion

In conclusion, the synthesis of three different model Xe biosensors was attempted on a solid support by selectively incorporating one of the crytophane-A derivatives (CryA-da, CryA-ma) onto the backbone. The first biosensor was generated with rather low yield due to incomplete reaction of the two larger building blocks. However, the second biosensor was successfully synthesized on the solid support by using submillimolar equivalents of CryA-da and by prolonging the coupling procedure. Additionally, ^{129}Xe-HyperCEST spectra indicated that CryA-da is still able to produce ca. 50 % CEST intensity despite of being tethered on both sides to other units. Further, this biosensor produced ^{129}Xe-HyperCEST images with reasonable contrast compared to the reference of freely acceessible CryA-ma. However, the synthesis of model biosensor with all functional units installed on the side chains resulted majorly in a peptide backbone without any CryA label.

The protocol introduced here will be helpful to facilitate new sensors in the expanding field of Xe MRI applications. A similar type of Xe biosensor was utilized earlier [24] in combination with antibodies for specifically labeling the CD14-expressing macrophage cell line via the modular approach. Therefore, such biosensors hold potential as building blocks for generating highly sensitive probes for visualizing otherwise MRI-inaccessible biological targets *in vivo*. The use of CryA-da enables the synthesis of compact sensors with minimized risk of peptide-cage interactions that could restrict Xe accessibility to the cavity. Furthermore, the generation of new biosensors on the solid support can be fostered by utilizing monoprotected CryA-da for selective and straightforward installation of different labels. This also illustrates a growing importance of CryA-da-based Xe biosensors for achieving different biomedical applications which might open up a broad interest in the synthesis and optimization of new CryA-da-based derivatives.

Supporting Information Available

MALDI-MS data, HPLC chromatograms, DLS data and ^{129}Xe-HyperCEST images

Author contributions

Manuscript was prepared by contributions from all authors.

Notes

The authors declare no competing financial interest.

Acknowledgement

The authors would like to thank Ms. Kristina Siebertz and Dr. Jan Oliver Jost for their fruitful discussion and MSc Hen Amit Morik for his help with the imaging experiments. Financial support from the Deutsche Forschungsgemeinschaft (DFG) through the Koselleck Grant SCHR 995/5-1 is gratefully acknowledged.

References

(1) Lippert, A. R., Keshari, K. R., Kurhanewicz, J., and Chang, C. J. (2011) A Hydrogen Peroxide-Responsive Hyperpolarized ^{13} C MRI Contrast Agent. *J. Am. Chem. Soc. 133*, 3776–3779.

(2) Vuichoud, B., Milani, J., Bornet, A., Melzi, R., Jannin, S., and Bodenhausen, G. (2014) Hyperpolarization of Deuterated Metabolites via Remote Cross-Polarization and Dissolution Dynamic Nuclear Polarization. *J. Phys. Chem. B 118*, 1411–1415.

(3) Shchepin, R. V., Barskiy, D. A., Mikhaylov, D. M., and Chekmenev, E. Y. (2016) Efficient Synthesis of Nicotinamide-1- ^{15} N for Ultrafast NMR Hyperpolarization Using Parahydrogen. *Bioconjugate Chem. 27*, 878–882.

(4) Shchepin, R. V., Truong, M. L., Theis, T., Coffey, A. M., Shi, F., Waddell, K. W., Warren, W. S., Goodson, B. M., and Chekmenev, E. Y. (2015) Hyperpolarization of "Neat" Liquids by NMR Signal Amplification by Reversible Exchange. *J. Phys. Chem. Lett. 6*, 1961–1967.

(5) Spence, M. M., Rubin, S. M., Dimitrov, I. E., Ruiz, E. J., Wemmer, D. E., Pines, A., Yao, S. Q., Tian, F., and Schultz, P. G. (2001) Functionalized xenon as a biosensor. *Proc Natl Acad Sci USA 98*, 10654–10657.

(6) Schröder, L., Lowery, T. J., Hilty, C., Wemmer, D. E., and Pines, A. (2006) Molecular Imaging Using a Targeted Magnetic Resonance Hyperpolarized Biosensor. *Science 314*, 446–449.

(7) Luhmer, M., Goodson, B. M., Song, Y.-Q., Laws, D. D., Kaiser, L., Cyrier, M. C., and Pines, A. (1999) Study of Xenon Binding in Cryptophane-A Using Laser-Induced NMR Polarization Enhancement. *J. Am. Chem. Soc. 121*, 3502–3512.

(8) Kunth, M., Witte, C., Hennig, A., and Schröder, L. (2015) Identification, classification, and signal amplification capabilities of high-turnover gas binding hosts in ultra-sensitive NMR. *Chem. Sci. 6*, 6069–6075.

(9) Bartik, K., Luhmer, M., Heyes, S. J., Ottinger, R., and Reisse, J. (1995) Probing Molecular Cavities in α-Cyclodextrin Solutions by Xenon NMR. *J. Magn. Reson. 109*, 164–168.

(10) Schnurr, M., Joseph, R., Naugolny-Keisar, A., Kaizerman-Kane, D., Bogdanoff, N., Schünke, P., Cohen, Y., and Schröder, L. (2018) High exchange rate complexes of 129Xe with water-soluble pillar[5]arenes for adjustable magnetization transfer MRI. *ChemPhysChem 19*, 1–7.

(11) Jeong, K., Netirojjanakul, C., Munch, H. K., Sun, J., Finbloom, J. A., Wemmer, D. E., Pines, A., and Francis, M. B. (2016) Targeted Molecular Imaging of Cancer Cells Using MS2-Based (129)Xe NMR. *Bioconjugate Chem. 27*, 1796–1801.

(12) Palaniappan, K. K., Ramirez, R. M., Bajaj, V. S., Wemmer, D. E., Pines, A., and Francis, M. B. (2013) Molecular Imaging of Cancer Cells Using a Bacteriophage-Based 129Xe NMR Biosensor. *Angew. Chem. Int. Ed. 52*, 4849–4853.

(13) Carrico, Z. M., Farkas, M. E., Zhou, Y., Hsiao, S. C., Marks, J. D., Chokhawala, H., Clark, D. S., and Francis, M. B. (2012) N-Terminal Labeling of Filamentous Phage To Create Cancer Marker Imaging Agents. *ACS Nano 6*, 6675–6680.

(14) Klippel, S., Döpfert, J., Jayapaul, J., Kunth, M., Rossella, F., Schnurr, M., Witte, C., Freund, C., and Schröder, L. (2014) Cell Tracking with Caged Xenon: Using Cryptophanes as MRI Reporters upon Cellular Internalization. *Angew. Chem. Int. Ed. 53*, 493–496.

(15) Klippel, S., Freund, C., and Schröder, L. (2014) Multichannel MRI Labeling of Mammalian Cells by Switchable Nanocarriers for Hyperpolarized Xenon. *Nano Lett. 14*, 5721–5726.

(16) Westmeyer, G. G., Truong, D.-J. J., Schröder, L., Rossella, F., and Witte, C. Molecular sensor for NMR/MRI based on analyte-dependent spectral changes of temporarily encapsulated hyperpolarized 129Xe. patent WO 2018/020025 A1, 2018.

(17) Riggle, B. A., Greenberg, M. L., Wang, Y., Wissner, R. F., Zemerov, S. D., Petersson, E. J., and Dmochowski, I. J. (2017) A cryptophane-based "turn-on" 129Xe NMR biosensor for monitoring calmodulin. *Org. Biomol. Chem. 15*, 8883–8887.

(18) Brotin, T., Berthault, P., Boutin, C., Jeanneau, E., and Léonce, E. (2017) Role of the Methoxy Groups in Cryptophanes for Complexation of Xenon Conformational Selection Evidenced by 129Xe-1H NMR SPINOE Experiments. *ChemPhysChem 18*, 1561–1568.

(19) Khan, N. S., Riggle, B. A., Seward, G. K., Bai, Y., and Dmochowski, I. J. (2015) Cryptophane-Folate Biosensor for 129Xe NMR. *Bioconjugate Chem. 26*, 101–109.

(20) Seward, G. K., Wei, Q., and Dmochowski, I. J. (2008) Peptide-Mediated Cellular Uptake of Cryptophane. *Bioconjugate Chem. 19*, 2129–2135.

(21) Zemerov, S. D., Roose, B. W., Greenberg, M. L., Wang, Y., and Dmochowski, I. J. (2018) Cryptophane Nanoscale Assemblies Expand 129Xe NMR Biosensing. *Anal. Chem. 90*, 7730–7738.

(22) Taratula, O., and Dmochowski, I. J. (2010) Functionalized 129Xe contrast agents for magnetic resonance imaging. *Curr. Opin. Chem. Biol. 14*, 97.

(23) Huber, G., Brotin, T., Dubois, L., Desvaux, H., Dutasta, J.-P., and Berthault, P. (2006) Water Soluble Cryptophanes Showing Unprecedented Affinity for Xenon:Candidates as NMR-Based Biosensors. *J. Am. Chem. Soc. 128*, 6239–6246.

(24) Rose, H. M., Witte, C., Rossella, F., Klippel, S., Freund, C., and Schröder, L. (2014) Development of an antibody-based, modular biosensor for 129Xe NMR molecular imaging of cells at nanomolar concentrations. *Proc Natl Acad Sci USA 111*, 11697–11702.

(25) Seward, G. K., Bai, Y., Khan, N. S., and Dmochowski, I. J. (2011) Cell-compatible, integrin-targeted cryptophane-129Xe NMR biosensors. *Chem Sci 2*, 1103–1110.

(26) Augustyns, K., Kraas, W., and Jung, G. (1998) Investigation on the stability of the Dde protecting group used in peptide synthesis: migration to an unprotected lysine. *J. Pept. Res. 51*, 127–133.

(27) Tyagi, R., Witte, C., Haag, R., and Schröder, L. (2014) Dendronized Cryptophanes as Water-Soluble Xenon Hosts for 129Xe Magnetic Resonance Imaging. *Org. Lett. 16*, 4436–4439.

Graphical TOC Entry